NEW COMPLEX *KMT2A-R* INVOLVING CHROMOSOMES 11, 16 AND 19 IN A CHILD WITH ACUTE MYELOID LEUKEMIA/MYELOID SARCOMA ASSOCIATED WITH OVEREXPRESSION OF *MLLT1* AND *ELL*

ROBERTO R. CAPELA DE MATOS (DO)[1,2], DANIELA R. NEY GARCIA[1,2,3], MARIANA TAVARES DE SOUZA[1,2], GERSON MOURA FERREIRA[4], KELLY MONTESO[1,2], MARCELO G. P. LAND[3], RAUL C. RIBEIRO[5], MARIA LUIZA MACEDO SILVA[1,2]

[1.] Cytogenetics Department, Bone Marrow Transplantation Unit, Instituto Nacional de Câncer José Alencar Gomes da Silva (INCA), Rio de Janeiro, Brazil; [2]. Post-Graduate Program in Oncology, Instituto Nacional de Câncer José Alencar Gomes da Silva (INCA), Rio de Janeiro, Brazil; [3]. Clinical Medicine Post-Graduation Program, College of Medicine, Federal University of Rio de Janeiro (UFRJ), Rio de Janeiro, Brazil; [4]. Stem Cells Department, Bone Marrow Transplantation Unit, Instituto Nacional Câncer José de Alencar Gomes da Silva (INCA), Rio de Janeiro, Brazil; [5]. Instituto Pelé Pequeno Príncipe, Postgraduate Program in Child Adolescent Health.

INTRODUCTION

Myeloid neoplasms are a group of heterogeneous hematological disorders that diverge in cell differentiation, proliferation and clinical course. Pediatric patients with acute myeloid leukemia (AML) presenting complex karyotypes have a dismal outcome. However, the prognosis for leukemia with a *KMT2A* rearrangements appear to mainly depend on the fusion partner gene. Thus, a precise characterization of *KMT2A*-r and its fusion partner genes, especially in complex karyotypes, are of interest for managing childhood AML.

In this doctoral project, we aim to detect and characterize complex karyotypes by combining conventional cytogenetic techniques and molecular approaches to better define and understand their biological role in pediatric AML.

In this context, herein, we describe the clinical and molecular features of a child with AML who presented with a large abdominal mass and a new complex chromosomal abnormality involving chromosomes 11, 16, and 19, leading to a *KMT2A-MLLT1* and two extra copies of the *ELL* gene, resulting in overexpression of *MLLT1* and *ELL*.

EXPERIMENTAL DESIGN

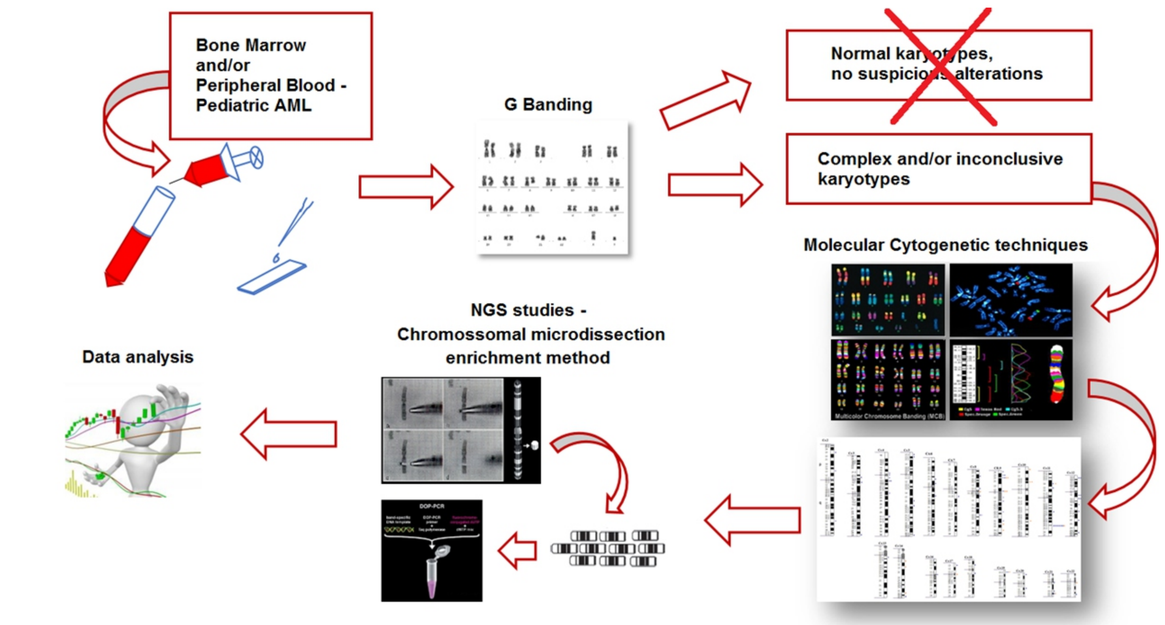

*This project was approved by the research ethics committee of INCA (#088/07)

METHODS AND RESULTS

Patient

A 7-year-old boy presented to the university hospital, Instituto de Puericultura e Pediatria Martagão Gesteira (IPPMG), Rio de Janeiro, Brazil, with a 3-week history of progressive abdominal distention and pain associated with generalized jaundice. On physical examination, adenomegaly, scrotal edema and diffuse gingival hypertrophy were observed. Also, a large abdominal mass was palpable in the epigastric and mesogastric regions.

Laboratory data showed hemoglobin level of 9.8 g/dL, a white blood cell count of 2.5 × 10^9/L, and a platelet count of 182 × 10^9/L. LDH was 4,860 U/L. The total bilirubin level was 7.5 mg/dL, and the direct bilirubin level was 6.4 mg/dL. Abdominal ultrasound scan showed an abdominal mass contiguous with the head of the pancreas, measuring 7.0 cm × 6.5 cm. A computed tomography examination confirmed the presence of an abdominal mass compressing the midline structures, a myeloid sarcoma (MS) (**Figure 1**). Bone marrow aspirate was hypercellular, with 75% of leukemia monoblastic cells.

Flow cytometry analysis revealed a population of leukemic blast cells that expressed $CD33^{+/++}$, $CD36^{-/+(27\%)}$, $CD45^{+low}$, $CD117^{-/++(45\%)}$, $CD64^{+}$, $HLA\text{-}DR^{+++}$, $CD71^{+/++}$, and $cyMPO^{+}$ and were negative for CD34, CD19, CD10, CD79, CD7, cyCD3, CD3, CD13, CD11b, CD35, nuTdT, CD105, IREM2, CD14, CD56, and CD16, corroborating the diagnosis of acute monoblastic leukemia. The patient was treated in accordance with a high-risk AML-BFM2012 protocol.

The child experienced morphologic remission on day 27; however, minimal residual disease (MRD) remained positive (0.5% and 0.3% blast cells). Eleven months after the diagnosis, MRD was negative. The patient remains in continuous complete remission. Although this patient had a high risk of relapse, a suitable bone marrow donor was not identified.

Conventional Cytogenetics

Cytogenetic analysis was performed at diagnosis, before treatment administration, in bone marrow samples cultured for 24 hours according to the standard protocol.

Molecular Assays

Fluorescence *in situ* hybridization-based experiments were conducted using both, homemade and commercial probes, according to the manufacturers' instructions. aCGH was performed in accordance with standard procedures. LDI-PCR assays were performed to identify the *KMT2A* partner genes and the corresponding breakpoints. RT-qPCR analyses were performed to verify levels of transcript expression of putative genes involved in the rearrangement.

Results

G-banded analysis showed a karyotype with 47 chromosomes, 11q23 region involvement, and the derivative chromosomes der(16) and der(19), along with a marker chromosome (**Figure 2A**). Molecular cytogenetic studies defined the karyotype as: 47,XY,der(11)t(11;16)(q23.3;p11.2),der(16)t(16;19)(p11.2;p13.3),der(19)t(11;19)(q23.3;p13.3),+der(19)t(16;19)(16pter->p11.2::19p13.3->19q11::19p11->19p13.3::16p11.2->16pter). (**Figure 2B**).

aCGH revealed a gain of 30.5 Mb in the region of 16p13.3-p11.2, and a gain of 18.1 Mb in the region of 19p13.3-p12 (**Figure 2C-D**). LDI-PCR showed the KMT2A-MLLT1 fusion. (**Figure 2E**).

Reverse sequence analysis showed that the MLLT1 gene was fused to 16p11.2 region. RT-qPCR quantification revealed that both ELL and MLLT1 were overexpressed (4 and 10 fold respectively). (**Figure 2F**).

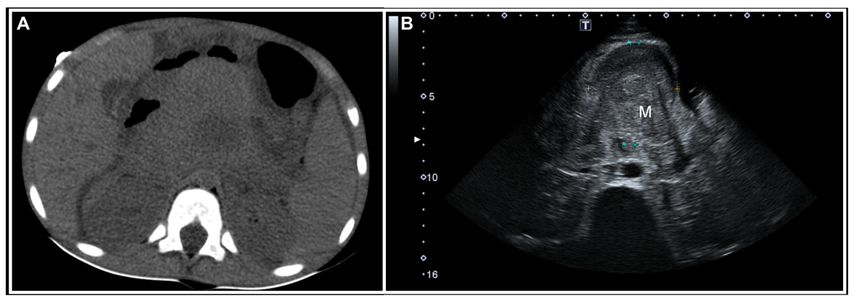

Figure 1: Clinical diagnostic data of MS and AML. **A)** Transverse focal CT image of the mesogastric region, acquired without contrast and with low ionizing irradiation, showing an expansive solid mass (M) on the midline with sharp margin definition and occupying the superior quadrants of the right mesogastrium. The mass extends through the hepatic hilum and the cleavage plane of the pancreas head. Li: liver; Sp; spleen. **B)** Ultrasonography image showing the extent (A+/+) of a solid mass (M: 7 cm × 6.5 cm) with characteristics compatible with the CT image. RK: right kidney; Ao: aorta; IVC: inferior vena cava.

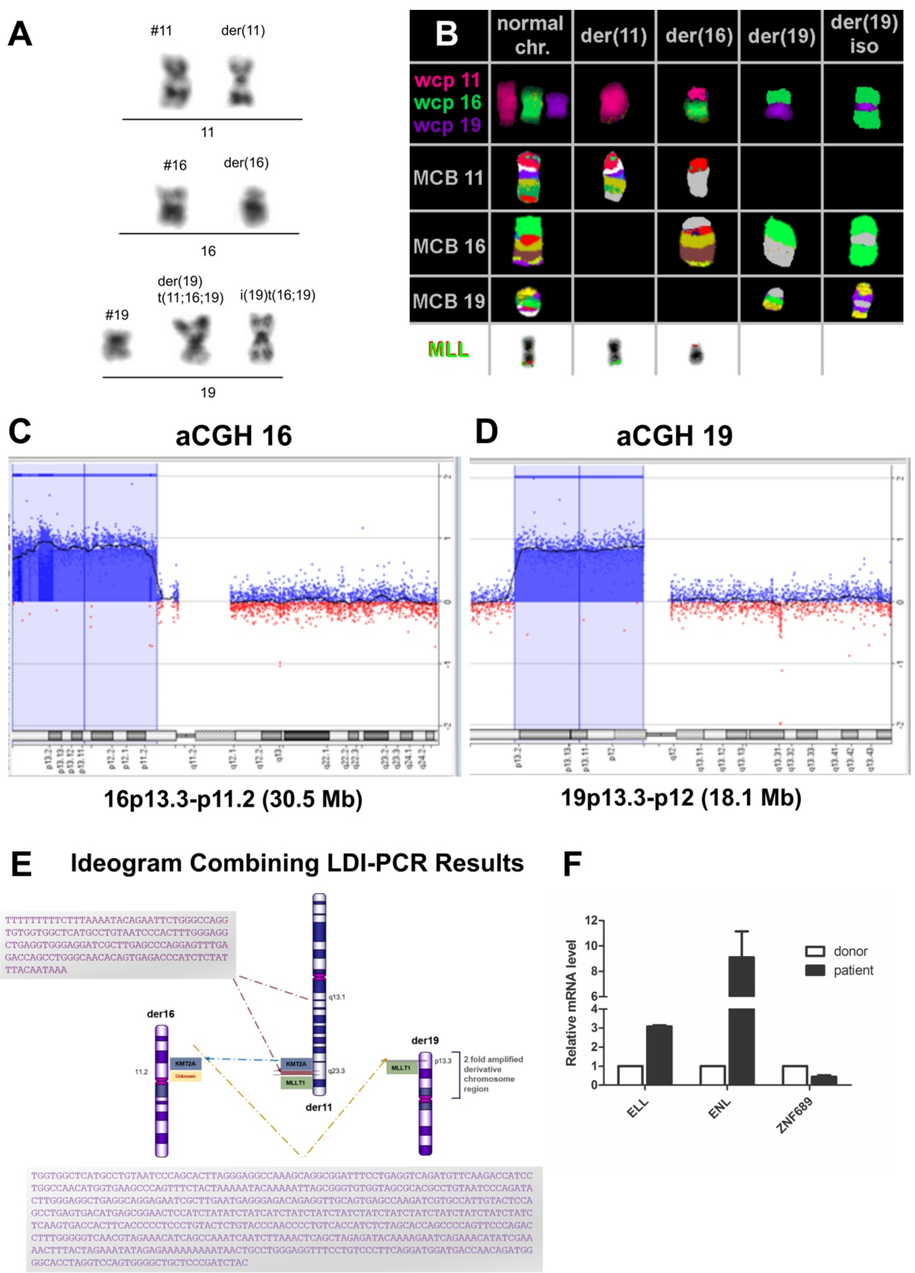

Figure 2: Results of cytogenetic and molecular studies. **A)** Partial karyotype showing derivatives (der) of chromosomes 11 and 16 and two derivatives of chromosome 19. Normal chromosomes (#) are also shown. **B)** Molecular cytogenetic analysis using whole-chromosome painting for chromosomes 11 (pink), 16 (green), and 19 (purple), showing one normal copy of each chromosome and the chromosomal composition of the derivative chromosomes. The MCB results obtained using probes for chromosomes 11, 16, and 19 determine the breakpoints of all the derivatives; the corresponding nonhybridized regions are depicted in gray. **C-D)** aCHG results. Left: aCGH16 shows a gain of 30.5 Mb in the region of 16p13.3-p11.2, narrowing down the breakpoint to 30,660,848. Right: aCGH19 shows a gain of 18.1 Mb in the region of 19p13.3-p12, mapping this breakpoint to position 24,378,493. **E)** Ideogram representing the final results, combining the results of all experimental approaches, including LDI-PCR. An unidentified (unknown) sequence from the 11q13 chromosome region was present between the fused KMT2A intron11 and MLLT1 intron6. The reverse MLLT1 (intron6) sequence was fused to the 16p11.2-region sequence. No reciprocal X-KMT2A fusion was found. **F)** Relative expression of ELL, ENL (MLLT1), and ZNF689 in the patient, as compared with the average values for three healthy donors. Data are presented as the mean ± standard deviation for three independent experiments.

CONCLUSION

This unreported unbalanced karyotype resulted in a large triplication of the region comprising the *ELL* gene, as in the formation of the isochromosome der(19)t(16;19), with four copies of the *ELL* gene being present in this abnormal genome.

Therefore, in our patient, the overexpression of *ELL* and *MLLT1* was probably associated with different mechanisms.

Regarding the clinical presentation with signs and symptoms of a myeloid sarcoma, as it usually occurs in association with karyotypes that reflect favorable outcomes, it is unlikely to be an independent prognostic indicator.

Overall, we contribute to the literature with the description of a pediatric case of AML presenting a novel complex t(11;16;19) variant associated with overexpression of *ELL*, and *MLLT1*.

ACKNOWLEDGEMENTS

The authors acknowledge with gratitude Mariana Tavares de Souza, MSc, for her contributions to cytogenetics discussions, Dr. Claudia Silva for providing tomography and ultrasonography images, Dr. Kelly Monteso for case discussion, Alice Theophilo Teixeira de Matos for editing the figures.

This work was supported by PROBRAL (DAAD No. 419/14), and FAPERJ (project No. E-26/110: 868/2013 and E-26/200.50/2016), INCT Para o Controle do Câncer, the St. Jude Children's Research Hospital (Memphis, Tenn., USA) and Center of Excellence Grant, Tenn., USA.

Projeto Gráfico: Área de Edição e Produção de Materiais Técnico-Científicos / INCA